

# Compressed modes for variational problems in mathematics and physics

Vidvuds Ozoliņš<sup>a,1</sup>, Rongjie Lai<sup>b,1</sup>, Russel Caflisch<sup>c,1</sup>, and Stanley Osher<sup>c,1,2</sup>

Departments of <sup>a</sup>Materials Science and Engineering, and <sup>c</sup>Mathematics, University of California, Los Angeles, CA 90095-1555; and <sup>b</sup>Department of Mathematics, University of California, Irvine, CA 92697-3875

Contributed by Stanley Osher, October 8, 2013 (sent for review September 3, 2013)

**This article describes a general formalism for obtaining spatially localized (“sparse”) solutions to a class of problems in mathematical physics, which can be recast as variational optimization problems, such as the important case of Schrödinger’s equation in quantum mechanics. Sparsity is achieved by adding an  $L_1$  regularization term to the variational principle, which is shown to yield solutions with compact support (“compressed modes”). Linear combinations of these modes approximate the eigenvalue spectrum and eigenfunctions in a systematically improvable manner, and the localization properties of compressed modes make them an attractive choice for use with efficient numerical algorithms that scale linearly with the problem size.**

Significant progress has been recently achieved in a variety of fields of information science using ideas centered around sparsity. Examples include compressed sensing (1, 2), matrix rank minimization (3), phase retrieval (4), and robust principal component analysis (5), as well as many others. A key step in these examples is use of a variational formulation with a constraint or penalty term that is an  $\ell_1$  or related norm. A limited set of extensions of sparsity techniques to physical sciences and partial differential equations (PDEs) have also appeared recently, including numerical solution of PDEs with multiscale oscillatory solutions (6) and efficient materials models derived from quantum mechanics calculations (7). In all of these examples, sparsity is for the coefficients (i.e., only a small set of coefficients are nonzero) in a well-chosen set of modes (e.g., a basis or dictionary) for representation of the corresponding vectors or functions. In this article, we propose a use of sparsity-promoting techniques to produce “compressed modes” (CMs)—modes that are sparse and localized in space—for efficient solution of constrained variational problems in mathematics and physics.

Our idea is motivated by the localized Wannier functions developed in solid state physics and quantum chemistry. We begin by reviewing the basic ideas for obtaining spatially localized solutions of the independent-particle Schrödinger’s equation. For simplicity, we consider a finite system with  $N$  electrons and neglect the electron spin. The ground state energy is given by  $E_0 = \sum_{j=1}^N \lambda_j$ , where  $\lambda_j$  are the eigenvalues of the Hamiltonian,  $\hat{H} = -\frac{1}{2}\Delta + V(\mathbf{x})$ , arranged in increasing order and satisfying  $\hat{H}\phi_j = \lambda_j\phi_j$ , with  $\phi_j$  being the corresponding eigenfunctions. This can be recast as a variational problem requiring the minimization of the total energy subject to orthonormality conditions for wave functions:

$$E_0 = \min_{\Phi_N} \sum_{j=1}^N \langle \phi_j, \hat{H}\phi_j \rangle \quad \text{s.t.} \quad \langle \phi_j, \phi_k \rangle = \delta_{jk}. \quad [1]$$

Here,  $\Phi_N = \{\phi_j\}_{j=1}^N$  and  $\langle \phi_j, \phi_k \rangle = \int_{\Omega} \phi_j^*(\mathbf{x})\phi_k(\mathbf{x}) \, d\mathbf{x} (\Omega \subset \mathbb{R}^d)$ .

In most cases, the eigenfunctions  $\phi_j$  are spatially extended and have infinite support—that is, they are “dense.” This presents challenges for computational efficiency [as the wave function orthogonalization requires  $O(N^3)$  operations, dominating the computational effort for  $N \approx 10^3$  electrons and above] and is contrary to physical intuition, which suggests that the screened correlations in condensed matter are usually short-ranged (8). It is well understood

that the freedom to choose a particular unitary transformation (“subspace rotation”) of the wave functions  $\phi_j$  can be used to define a set of functions that span the eigenspace of  $\hat{H}$ , but are spatially localized or sparse. Methods for obtaining such functions have been developed in solid state physics and quantum chemistry, where they are known as Wannier functions (9).

Mathematically, the Wannier functions are obtained as a linear combination of the eigenfunctions:

$$W_j(\mathbf{x}) = \sum_k U_{jk} \phi_k(\mathbf{x}), \quad [2]$$

where the subspace rotation matrix  $U$  is unitary,  $U^\dagger U = I$ . Currently, the most widely used approach to finding  $W_j(\mathbf{x})$  is the one proposed in ref. 10 for calculating maximally localized Wannier functions (MLWFs). This approach starts with the precalculated eigenfunctions  $\phi_j$  and determines  $W_j$  by minimizing the second moment:

$$\langle \Delta \mathbf{x}_j^2 \rangle = \langle W_j, (\mathbf{x} - \langle \mathbf{x}_j \rangle)^2 W_j \rangle, \quad [3]$$

where  $\langle \mathbf{x}_j \rangle = \langle W_j, \mathbf{x} W_j \rangle$ . More recently, a method weighted by higher degree polynomials has been discussed in ref. 11. Although this approach works reasonably well for simple systems, constructing optimally localized real-valued Wannier functions is often difficult because the minimization problem (Eq. 3) is nonconvex and requires a good starting point to converge to the global minimum. Another difficulty is that when the resulting MLWFs are used to construct efficient numerical algorithms, they need to be cut off “by hand,” which can result in significant numerical errors when the MLWFs are calculated “on the fly” and their range is not known in advance. It would be highly desirable to devise an approach that does not require the calculation of the eigenfunctions

## Significance

Intuition suggests that many interesting phenomena in physics, chemistry, and materials science are “short-sighted”—that is, perturbation in a small spatial region only affects its immediate surroundings. In mathematical terms, near-sightedness is described by functions of finite range. As an example, the so-called Wannier functions in quantum mechanics are localized functions, which contain all the information about the properties of the system, including its spectral properties. This work’s main research objective is to develop theory and numerical methods that can systematically derive functions that span the energy spectrum of a given quantum-mechanical system and are nonzero only in a finite spatial region. These ideas hold the key for developing efficient methods for solving partial differential equations of mathematical physics.

Author contributions: V.O. designed research; V.O., R.L., R.C., and S.O. performed research; and V.O. and R.L. wrote the paper.

The authors declare no conflict of interest.

<sup>1</sup>V.O., R.L., R.C., and S.O. contributed equally to this work.

<sup>2</sup>To whom correspondence should be addressed. E-mail: sjo@math.ucla.edu.

and would converge to localized functions, while simultaneously providing a variational approximation to the total energy  $E_0$ .

In this article, we propose a method to create a set of localized functions  $\{\psi_j\}_{j=1}^N$ , which we call CMs, such that  $\sum_{j=1}^N \langle \psi_j, \hat{H} \psi_j \rangle$  approximates  $E_0 = \sum_{j=1}^N \langle \phi_j, \hat{H} \phi_j \rangle$ . Our idea is inspired by the  $\ell_1$  regularization used in compressive sensing. As a convex relaxation of  $\ell_0$  regularization,  $\ell_1$  regularization is commonly used for seeking sparse solutions for the underdetermined problem  $Ax=b$  (2, 12). Motivated by advantages of the  $\ell_1$  regularization for the sparsity in the discrete case, we propose a modification of the objective functional given by Eq. 1, which can immediately obtain functions with compact support and calculate approximate total energy “in one shot,” without the need to calculate eigenfunctions. This is accomplished by introducing an  $L_1$  regularization of the wave functions:

$$E = \min_{\Psi_N} \sum_{j=1}^N \left( \frac{1}{\mu} |\psi_j|_1 + \langle \psi_j, \hat{H} \psi_j \rangle \right) \text{ s.t. } \langle \psi_j, \psi_k \rangle = \delta_{jk}, \quad [4]$$

where  $\Psi_N = \{\psi_j\}_{j=1}^N$  and the  $L_1$  norm is defined as  $|\psi_j|_1 = \int_{\Omega} |\psi_j| dx$ . For simplicity, we are requiring that the wave functions  $\psi_j$  are real; generalization to complex-valued wave functions, required to handle relativistic effects, is straightforward. The parameter  $\mu$  controls the tradeoff between sparsity and accuracy: larger values of  $\mu$  will give solutions that better minimize the total energy at the expense of more extended wave functions, whereas a smaller  $\mu$  will give highly localized wave functions at the expense of larger errors in the calculated ground state energy. Due to the properties of the  $L_1$  term, the functions that minimize Eq. 4 will have compact support. In contrast to other approaches that use manually imposed cutoff distances, the main advantage of our scheme is that one parameter  $\mu$  controls both the physical accuracy and the spatial extent, while not requiring any physical intuition about the properties of the solution. In other words, the wave functions  $\psi_j$  are nonzero only in those regions that are required to achieve a given accuracy for the total energy and are zero everywhere else. Furthermore, due to the fact that exponentially localized Wannier functions are known to exist, the solution to Eq. 4 will provide a good approximation to the true total energy of the system (in fact, it converges to  $E_0$  as  $\mu^{-2}$ ).

As a major contribution in this article, we propose localized CMs using an  $L_1$  regularized variational formula. In addition, we propose a numerical algorithm to solve the proposed nonconvex problem.

### Variational Model for Compressed Modes

**Free-Electron Case.** Consider a 1D free-electron case defined on  $[0, L]$  with periodic boundary conditions. Namely, the Schrödinger operator is  $\hat{H}_0 = -\frac{1}{2}\partial_x^2$ . It is clear that  $\hat{H}_0$  has eigenfunctions  $\frac{1}{\sqrt{L}} e^{i2\pi n x/L}$  with the corresponding eigenvalues  $2(\pi n/L)^2$ ,  $n=0, \pm 1, \pm 2, \dots$ . With a unitary transformation  $U_{mn} = \frac{1}{\sqrt{L}} e^{i2\pi n m/L}$ , one can construct quasi-localized orthonormal functions as

$$W_m = \frac{1}{L} \sum_n e^{i2\pi n(x-m)/L}. \quad [5]$$

Fig. 1 illustrates the real part of one of the resulting quasi-localized functions obtained from the above unitary transformation. It is evident that the resulting  $W_m$  are not even exponentially localized, as expected for metallic systems with continuous energy spectrum at zero temperature (8).

As an example, we can analytically check that the  $L_1$  regularization introduced in Eq. 4 can localize the resulting functions. Let's again consider the 1D free-electron model defined on  $[0, L]$  with the Schrödinger operator  $\hat{H}_0 = -\frac{1}{2}\partial_x^2$ . Then the lowest mode satisfies:

$$\begin{aligned} \psi_1 = \arg \min_{\psi} & \frac{1}{\mu} \int_{\Omega} |\psi| dx - \frac{1}{2} \int_{\Omega} \psi \partial_x^2 \psi dx \\ \text{s.t. } & \int_{\Omega} \psi(x) \psi(x) dx = 1. \end{aligned} \quad [6]$$

The solution of the above minimization problem will be a sparse solution—that is, the Dirac delta function when  $\mu \rightarrow 0$ —and will approach the first eigenfunction of  $\hat{H}$  when  $\mu \rightarrow \infty$ . Intuitively, we expect to be able to express the solution of Eq. 6 as an approximation to a truncated diffusion of Dirac delta function via the Schrödinger operator  $-\frac{1}{2}\partial_x^2$ , which is a compactly supported function. Indeed, the Euler-Lagrange equation corresponding to Eq. 6 is:

$$-\partial_x^2 \psi_1 + \frac{1}{\mu} \text{sign}(\psi_1) = \lambda \psi_1. \quad [7]$$

If we further assume that  $\psi_1$  is symmetric around  $x=L/2$ , the solution of Eq. 6 is:

$$\psi_1 = \begin{cases} \frac{1}{\lambda \mu} \left[ 1 + \cos(\sqrt{\lambda}(x-L/2)) \right] & \text{if } |x-L/2| \leq l, \\ 0 & \text{if } l \leq |x-L/2| \leq L \end{cases}, \quad [8]$$

where  $l = \pi/\sqrt{\lambda}$  and  $\lambda = (3\pi)^{2/5} \mu^{-4/5}$ . Here  $\psi_1$  has compact support  $[L/2-l, L/2+l]$  if  $\mu$  is small enough satisfying  $l = \pi/\sqrt{\lambda} < L$ . Note that  $\psi_1 = \partial_x \psi_1 = 0$  and  $\partial_x^2 \psi_1$  has a jump of  $-\mu^{-1}$  at the boundary  $x=l$  of the support of  $\psi_1$ , which are all consistent with Eq. 7. From this simple 1D example, it is clear that  $L_1$  regularization can naturally truncate solutions to the variational problem given by Eq. 6. Moreover, we also observe that the smaller  $\mu$  will provide a smaller region of compact support. Fig. 2 shows  $\psi_1$  for different values of  $\mu$ .

The 1D solution Eq. 8 can be generalized to dimension  $d > 1$ , as:

$$\psi_1 = \begin{cases} \frac{1}{\lambda \mu} \left( 1 - U_0^{-1} U(\sqrt{\lambda}|\mathbf{x} - \mathbf{x}_0|) \right) & \text{if } |\mathbf{x} - \mathbf{x}_0| \leq l. \\ 0 & \text{if } l \leq |\mathbf{x} - \mathbf{x}_0| \leq L \end{cases}, \quad [9]$$

in which  $\mathbf{x}_0$  is the center of the cube  $[0, L]^d$  and  $U(\mathbf{y}) = U(r = |\mathbf{y}|)$  (for  $\mathbf{y} \in \mathbb{R}^d$ ) is the solution of  $\Delta U = -U$ —that is:

$$r^2 \partial_r^2 U + (d-1)r \partial_r U + r^2 U = 0 \quad [10]$$

and  $U_0 = U(r_0)$ ,  $l = r_0/\sqrt{\lambda}$ ,  $\lambda = (\mu U_1)^{2/(d+2)}$ . Here  $r_0$  is the smallest (nonnegative) solution of  $\partial_r U(r) = 0$  and  $U_1 = \int_{|\mathbf{y}| < r_0} (1 - U_0^{-1} U(|\mathbf{y}|))^2 d\mathbf{y}$  in which  $\mathbf{y}$  is in  $\mathbb{R}^d$ . For  $d=2$ ,  $U(r) = J_0(r)$  is the 0-th Bessel function of the first kind, and for  $d=3$ ,  $U(r) = \text{sinc}(r) = \sin(r)/r$ .

**Generalization to Nonzero Potential.** The simple free-electron example inspires us to consider  $L_1$  regularization of the wave functions

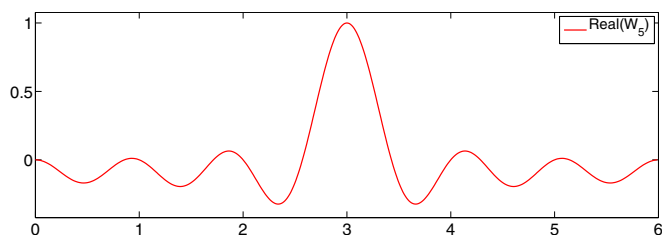


Fig. 1. A quasi-localized Wannier function for 1D Laplace operator.

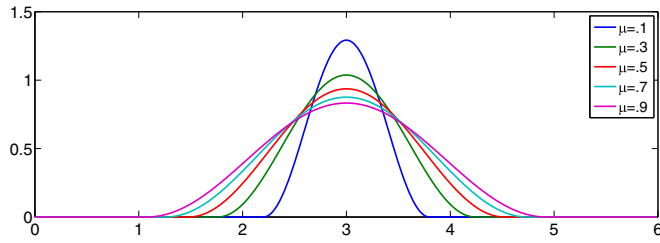


Fig. 2. Theoretical  $\psi_1$  in the 1D free-electron model (Eq. 6) for different values of  $\mu$ .

proposed in Eq. 4 for a general Schrödinger operator  $\hat{H} = -\frac{1}{2}\Delta + V(\mathbf{x})$  defined on  $\Omega \subset \mathbb{R}^d$ .

For definition 1, we call  $\Psi_N = \{\psi_1, \dots, \psi_N\}$ , defined in the variational model Eq. 4, the first  $N$  CMs of the Schrödinger operator  $\hat{H}$ .

By analogy with the localized Wannier functions described in the opening paragraphs, we expect that the CMs have compact support and can be expressed as orthonormal combinations of the eigenmodes of the original Schrödinger operator. In other words, let  $\Phi_M = \{\phi_1, \dots, \phi_M\}$  be the first  $M$  eigenfunctions of  $\hat{H}$  satisfying:

$$\hat{H}\Phi_M = \Phi_M \text{diag}(\lambda_1, \dots, \lambda_M) \quad \& \quad \int_{\Omega} \phi_j \phi_k \, d\mathbf{x} = \delta_{ij}. \quad [11]$$

We formulate the following conjecture to describe the completeness of the CMs. Given  $N \geq M$ , consider the  $N \times N$  matrix  $\langle \Psi_N^T, \hat{H}\Psi_N \rangle$  with the  $(j, k)$ -th entry defined by  $\int_{\Omega} \psi_j \hat{H}\psi_k \, d\mathbf{x}$  and let  $(\sigma_1, \dots, \sigma_M)$  be its first  $M$  eigenvalues; then:

$$\lim_{\mu \rightarrow \infty} \sum_{j=1}^M (\sigma_j - \lambda_j)^2 = 0 \quad \text{and} \quad \lim_{N \rightarrow \infty} \sum_{j=1}^M (\sigma_j - \lambda_j)^2 = 0. \quad [12]$$

## Numerical Algorithms

To numerically compute the proposed CMs, we consider the system on a domain  $D = [0, L]^d \subset \mathbb{R}^d$  with periodic boundary conditions and discretize the domain  $D$  with  $n$  equally spaced nodes in each direction. Then, the variational formula (Eq. 4) for the first  $N$  CMs can be reformulated and discretized as follows:

$$\Psi_N = \min_{\Psi \in \mathbb{R}^{n \times N}} \frac{1}{\mu} |\Psi| + \text{Tr}(\Psi^T \hat{H}\Psi) \quad \text{s.t.} \quad \Psi^T \Psi = I, \quad [13]$$

in which  $|\Psi|$  is the  $\ell_1$  norm of the matrix  $\Psi$ .

We solve this optimization problem by splitting orthogonality constraint (SOC) using the algorithm proposed in ref. 13. By introducing auxiliary variables  $Q = \Psi$  and  $P = \Psi$ , the above problem Eq. 6 is equivalent to the following constrained problem:

$$\min_{\Psi, P, Q} \frac{1}{\mu} |Q| + \text{Tr}(\Psi^T \hat{H}\Psi) \quad \text{s.t.} \quad Q = \Psi, P = \Psi, P^T P = I, \quad [14]$$

which can be solved by the SOC algorithm based on split Bregman iteration (14–16).

For algorithm 1, initialize  $\Psi_N^0 = P^0 = Q^0, b^0 = B^0 = 0$ ; while “not converged” do:

- 1)  $\Psi_N^k = \arg \min_{\Psi} \text{Tr}(\Psi^T \hat{H}\Psi) + \frac{\lambda}{2} \|\Psi - Q^{k-1} + b^{k-1}\|_F^2 + \frac{\lambda}{2} \|\Psi - P^{k-1} + B^{k-1}\|_F^2$
- 2)  $Q^k = \arg \min_Q \frac{1}{\mu} |Q| + \frac{\lambda}{2} \|\Psi_N^k - Q + b^{k-1}\|_F^2$
- 3)  $P^k = \arg \min_P \frac{\lambda}{2} \|\Psi_N^k - P + B^{k-1}\|_F^2$  s.t.  $P^T P = I$

$$4) b^k = b^{k-1} + \Psi_N^k - Q^k$$

$$5) B^k = B^{k-1} + \Psi_N^k - P^k.$$

Solutions to the minimization subproblems 1–3 can be expressed as follows:

$$(2\hat{H} + \lambda + r)\Psi_N^k = r(P^{k-1} - B^{k-1}) + \lambda(Q^{k-1} - b^{k-1}), \quad [15]$$

$$Q^k = \text{Shrink}(\Psi_N^k + b^{k-1}, 1/(\lambda\mu)), \quad [16]$$

and

$$P^k = (\Psi_N^k + B^{k-1})U\Lambda^{-1/2}S^T, \quad [17]$$

where  $U\Lambda S^T = \text{svd}((\Psi^k + B^{k-1})^T(\Psi^k + B^{k-1}))$  and the “Shrink” (or soft-thresholding) operator is defined as  $\text{Shrink}(u, \delta) = \text{sgn}(u)\max(0, |u| - \delta)$ . Because the matrix  $2\hat{H} + \lambda + r$  in Eq. 15 is sparse and positive definite, in practice a few iterations of either Gauss–Seidel or conjugate gradient are sufficient to achieve good convergence. Thus, Eqs. 15 and 16 can be solved very efficiently with long operation counts linearly dependent on  $N$ . The only time-consuming part in our algorithm is Eq. 17, which involves a singular value decomposition (SVD) factorization and can be straightforwardly solved with an  $O(N^3)$  algorithm. For a moderate size of  $N$ , the proposed algorithm can solve the problem efficiently.

For a large number of modes  $N$ , a possible approach to accelerating the computation is to use graphs processing unit (GPU)-based parallel processing to perform the SVD factorization in Eq. 17. Here, we propose another method to speed up the third step of the proposed algorithm, which takes advantage of the special structure of the solution. We find that each of the resulting functions  $\psi_1, \dots, \psi_N$  has compact support, so that the support of each  $\psi_i$  overlaps with only a finite number of its neighbors. This allows us to replace the full orthogonality constraint  $\Psi^T \Psi = I$  by a system of banded orthogonality constraints.

$$\int \psi_j \psi_k \, d\mathbf{x} = \delta_{jk}, \quad \begin{cases} j = 1, \dots, N \\ k = j, j \pm 1, \dots, j \pm p \end{cases}, \quad [18]$$

where  $p$  is the bandwidth. Thus, the  $O(N^3)$  algorithm for SVD factorization in Eq. 17 can be replaced by  $N$  factorizations of  $2p \times 2p$  matrices, which is an algorithm with  $8p^3 O(N)$  long operations.

## Numerical Results

We illustrate our scheme for two representative cases. The first is the free-electron model, which approximates the behavior of valence electrons in a metallic solid with weak atomic pseudopotentials; the potential function in the Schrödinger operator is simply set to zero. Because the allowed energy spectrum of free electrons is continuous in the limit of infinite system size, the conventional Wannier functions decay as an inverse power law. The second case is that of a periodic one-dimensional crystal, of which the famous Kronig–Penney (KP) model (17) is the most widely used example. The KP model describes the states of independent electrons in a one-dimensional crystal, where the potential function  $V(\mathbf{x})$  consists of a periodic array of rectangular potential wells. For simplicity, in our experiments we replace the rectangular wells with inverted Gaussians so that the potential is given by  $V(x) = -V_0 \sum_{j=1}^{N_{\text{el}}} \exp\left[-\frac{(x-x_j)^2}{2\delta^2}\right]$ . We choose  $N_{\text{el}} = 5$ ,  $V_0 = 1$ ,  $\delta = 3$ , and  $x_j = 10j$  in our discussion below and, despite the different potential, continue to refer to this case as the 1D KP model. This model exhibits two low-energy bands separated by finite gaps from the rest of the (continuous) eigenvalue spectrum, and the Wannier functions corresponding to these bands are exponentially localized.

In our experiments, we choose  $\Omega = [0, 50]$  and discretize  $\Omega$  with 128 equally spaced nodes. The proposed variational model Eq. 4 is solved using algorithm 1, where parameters are chosen as



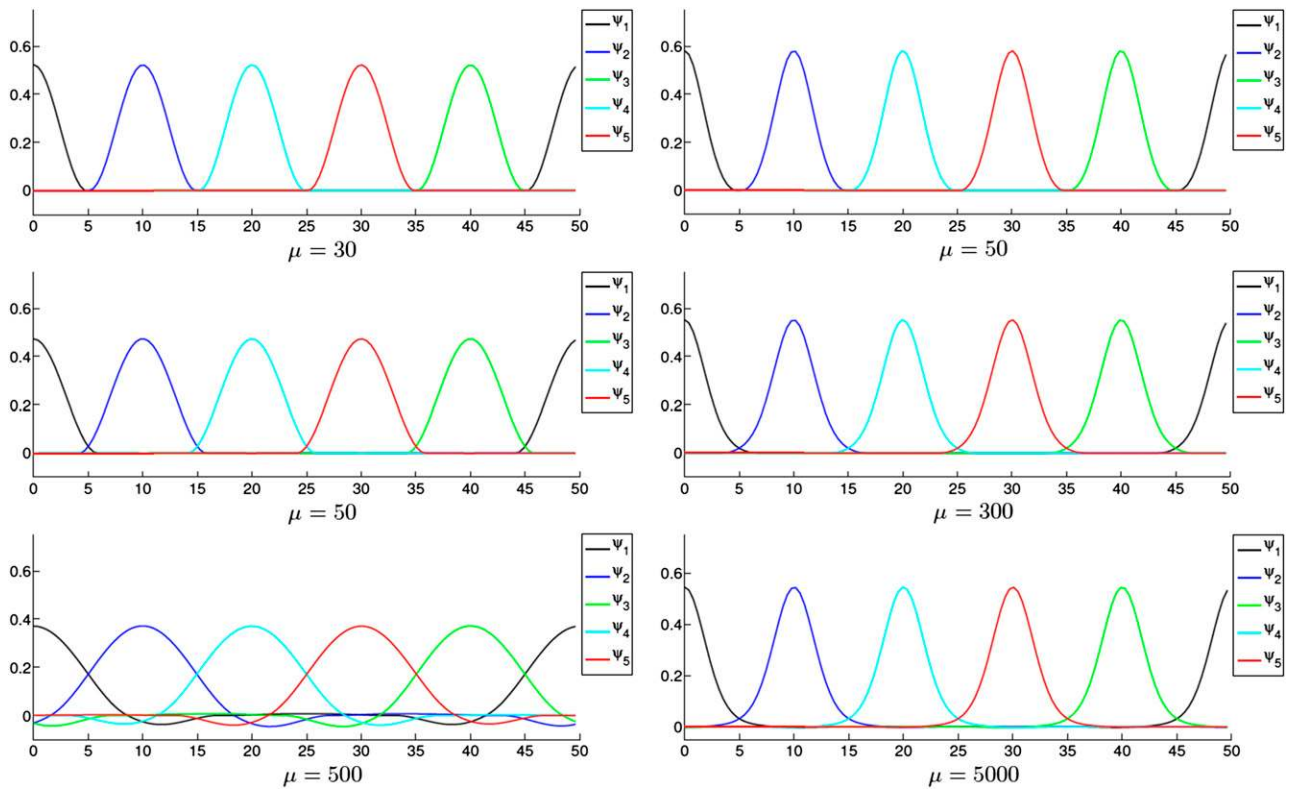


**Fig. 3.** Computation results of CMs with different values of  $\mu$ . The first column, the first five CMs of the 1D free-electron model; the second column, the first five CMs of the 1D KP model.

$\lambda = \mu N / 20$  and  $r = \mu N / 5$ . We report the computational results of the first five CMs of the 1D free-electron model (the first column) and the 1D KP model (the second column) in Fig. 3, where we use five different colors to differentiate these CMs. To compare all results more clearly, we use the same initial input for different values of  $\mu$  in the free-electron model and the 1D KP model. We flip the CMs if necessary such that most values of

CMs on their support are positive, as sign ambiguities do not affect minimal values of the objective function in Eq. 4. For comparison, Fig. 4 plots the first five eigenfunctions of the Schrödinger operator used in the free-electron model and KP model. It is clear that all these eigenfunctions are spatially extended without any compact support. However, as we can observe from Fig. 3, the proposed variational model does provide

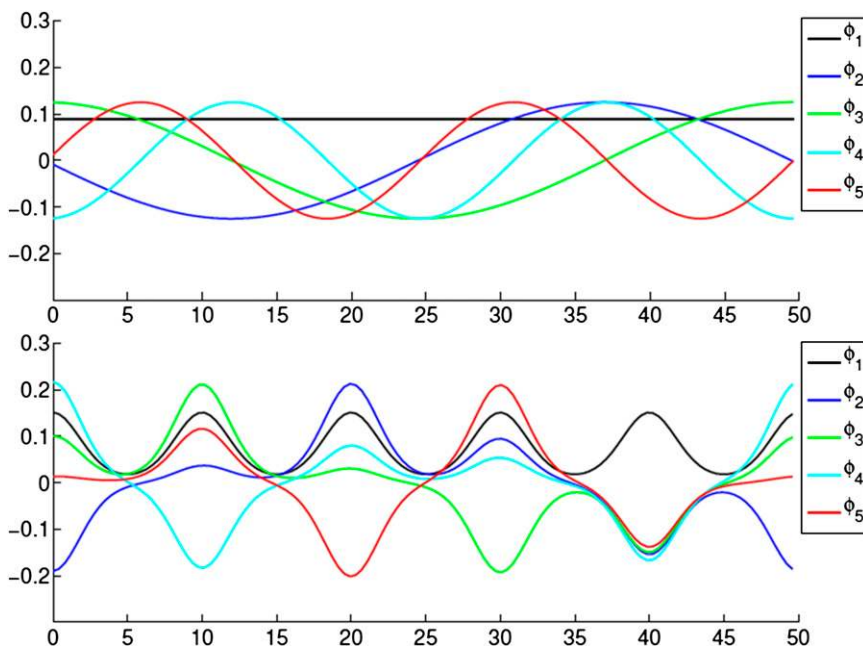


**Fig. 4.** The first five eigenfunctions of the Schrödinger operator  $\hat{H}$  in the free-electron model (Upper) and the KP model (Lower).

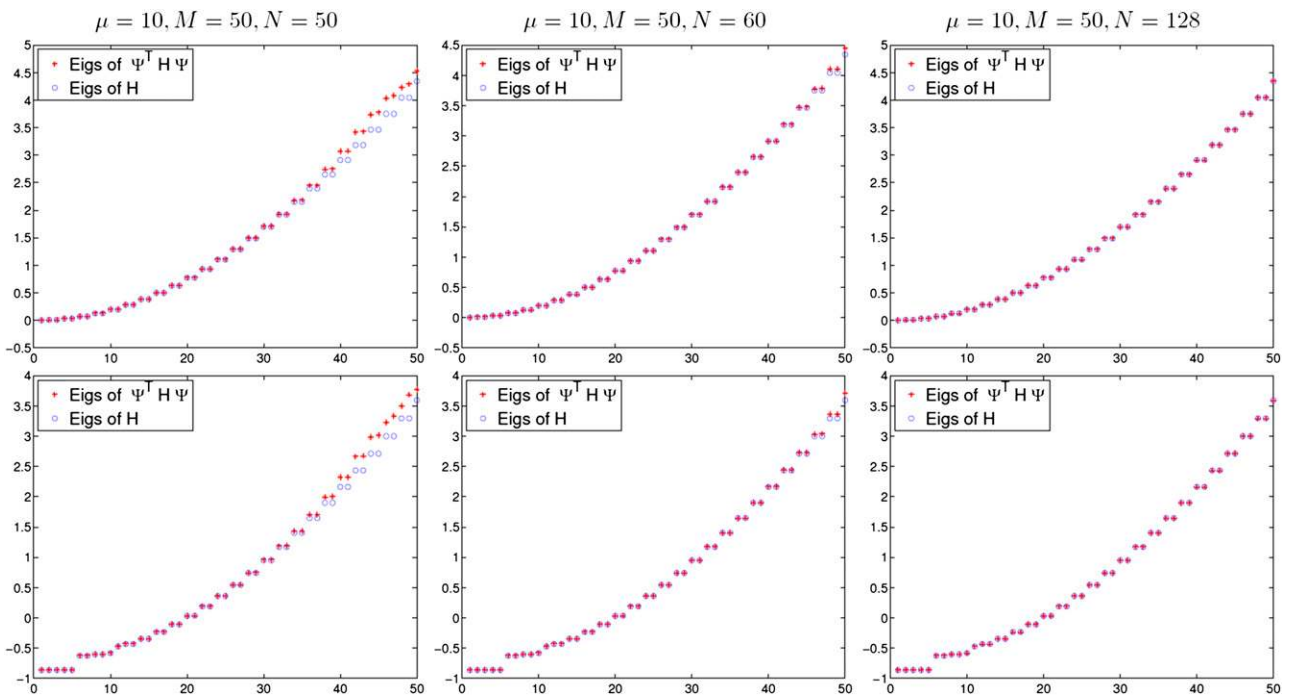


Fig. 5. Comparisons of the first 50 eigenvalues of the 1D free electron model (the first row) and the 1D KP model (the second row).

a series of compactly supported functions. Furthermore, all numerical results in Fig. 3 clearly show the dependence of the size of compact support on  $\mu$ , as suggested by general considerations based on the variational formula Eq. 4. In other words, the model with smaller  $\mu$  will create CMs with smaller compact support, and the model with larger  $\mu$  will create CMs with larger compact support. In addition, we find that the resulting CMs are not interacting for small  $\mu$  (the first row of Fig. 3). By increasing  $\mu$  to a moderate value, the modes start to interact with each other via a small amount of

overlap (the second row of Fig. 3). Significant overlap can be observed using a big value of  $\mu$  (the third row of Fig. 3).

We further test conjecture 1 (Eq. 12) numerically—that is, unitary transformation of the derived compactly supported CMs can represent the eigenmodes of the Schrödinger operator. We compare the first  $M$  eigenvalues  $(\sigma_1, \dots, \sigma_M)$  of the matrix  $\langle \Psi_N^T H \Psi_N \rangle$  obtained by the 1D KP model and 1D free-electron model with the first  $M$  eigenvalues  $(\lambda_1, \dots, \lambda_M)$  of the corresponding Schrödinger operators. Fig. 5 illustrates the comparisons with a

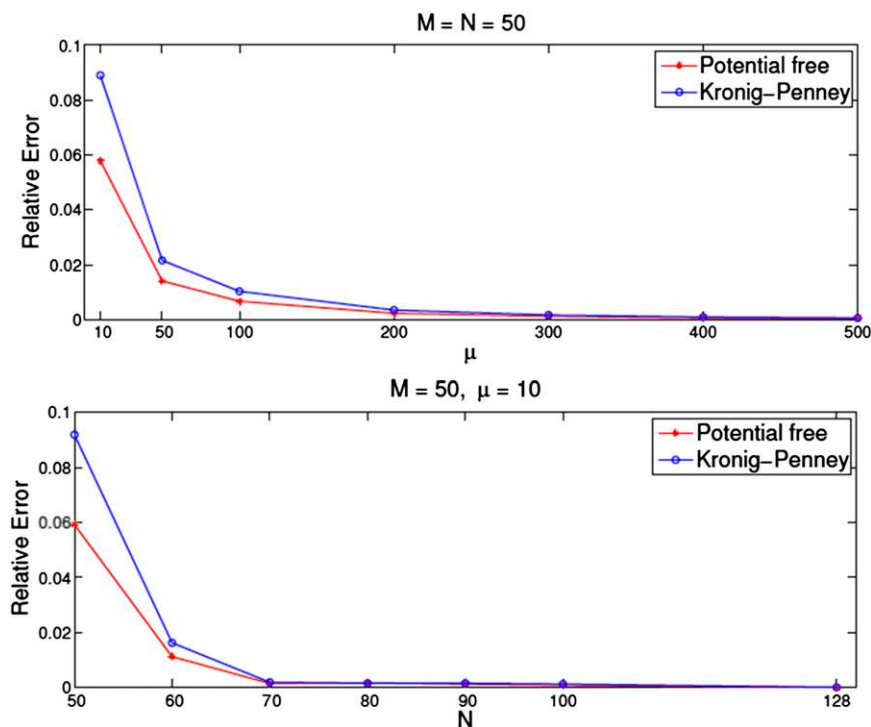


Fig. 6. Relative eigenvalue error of the 1D free-electron model (red dots) and 1D KP model (blue circles). (Upper) Relation of the relative error via different values of  $\mu$  for fixed  $M=N=50$ . (Lower) Relation of the relative error via different values of  $N$  for fixed  $\mu=10$  and  $M=50$ .

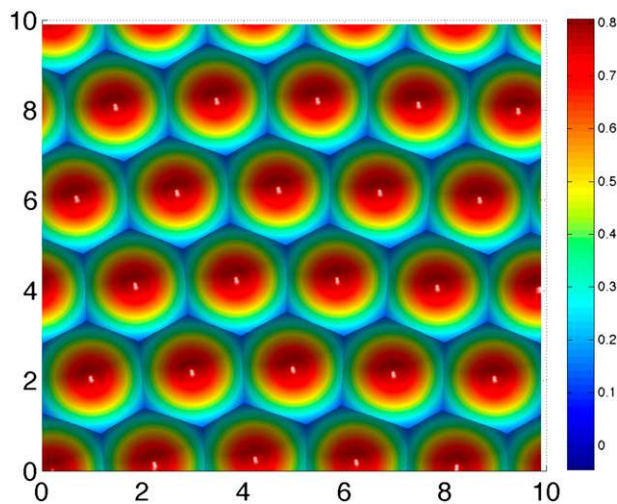


Fig. 7. The first 25 CMs of free-electron case on a 2D domain  $[0,10]^2$  with  $\mu=30$ . Each CM is color-coded by its height function.

relative small value  $\mu=10$ , when the CMs are highly localized. We can clearly see that  $\{\sigma_i\}$  gradually converges to  $\{\lambda_i\}$  with increasing number  $N$  of CMs. In addition, we also plot the relative error  $E = \sum_{i=1}^M (\sigma_i - \lambda_i)^2 / \sum_{i=1}^M (\lambda_i)^2$  in Fig. 6. As we speculated in conjecture 1, the relative error will converge to zero as  $\mu \rightarrow \infty$  for fixed  $M=N=50$ , which is illustrated in the upper panel of Fig. 6. The relative error will also converge to zero as  $N \rightarrow \infty$  for fixed  $\mu=10$  and  $M=50$ , which is illustrated in the lower panel of Fig. 6.

Moreover, the proposed model and numerical algorithm also work on domains in high dimensional space. As an example, Fig. 7 shows computational results of the first 25 CMs of the free-electron case on a 2D domain  $[0,10]^2$  with  $\mu=30$ . All of the above discussions of 1D model are also true for 2D cases. In addition, our approach can also be naturally extended to irregular domains, manifolds, as well as graphs, which will be investigated in our future work.

In conclusion, the above numerical experiments validate the conjecture that the proposed CMs provide a series of compactly supported orthonormal functions, which approximately span the low-energy eigenspace of the Schrödinger operator (i.e., the space of linear combinations of its first few lowest eigenmodes).

## Discussions and Conclusions

In conclusion, we have presented a method for producing CMs (i.e., modes that are sparse and spatially localized with a compact support) for the Laplace operator plus a potential  $V$ , using a variational principle with an  $L_1$  penalization term that promotes sparsity. The

tradeoff between the degree of localization and the accuracy of the variational energy is controlled by one numerical parameter,  $\mu$ , without the need for physical intuition-informed spatial cutoffs. The SOC algorithm of ref. 13 has been used to numerically construct these modes. Our tests indicate that the CMs can be used as an efficient, systematically improvable orthonormal basis to represent the low-energy eigenfunctions and energy spectrum of the Schrödinger operator. Due to the fact that the CMs are compactly supported, the computational effort of total energy calculations increases linearly with the number of modes  $N$ , overcoming the  $O(N^3)$  orthogonalization bottleneck limiting the performance of methods that work by finding the eigenfunctions of the Schrödinger operator.

In addition, note that the discretized variational principle in Eq. 13 is related to sparse principal component analysis (SPCA) (18, 19). SPCA, however, does not involve an underlying continuum variational principle, and the sparse principal components are not localized, as the component number does not correspond to a continuum variable.

These results are only the beginning. We expect that CM-related techniques will be useful in a variety of applications in solid state physics, chemistry, materials science, and other fields. Future studies could explore the following directions:

- i) Use CMs to develop spatially localized basis sets that span the eigenspace of a differential operator, for instance, the Laplace operator, generalizing the concept of plane waves to an orthogonal real-space basis with multiresolution capabilities. More details will be discussed in ref. 20.
- ii) Use the CMs to construct an accelerated [i.e.,  $O(N)$ ] simulation method for density-functional theory electronic structure calculations.
- iii) Construct CMs for a variety of potentials and develop CMs as the modes for a Galerkin method for PDEs, such as Maxwell's equations.
- iv) Generalize CMs for use in PDEs (such as heat type equations) that come from the gradient descent of a variational principle.
- v) Extend CMs to higher dimensions and different geometries, including the Laplace–Beltrami equation on a manifold and a discrete Laplacian on a network.

Finally, we plan to perform an investigation of the formal properties of CMs to rigorously analyze their existence and completeness, including the conjecture 1 (Eq. 12) that was hypothesized and numerically tested here.

**ACKNOWLEDGMENTS.** V.O. gratefully acknowledges financial support from the National Science Foundation under Award DMR-1106024 and use of computing resources at the National Energy Research Scientific Computing Center, which is supported by the US Department of Energy (DOE) under Contract DE-AC02-05CH11231. The research of R.C. is partially supported by the US DOE under Contract DE-FG02-05ER25710. The research of S.O. was supported by the Office of Naval Research Grant N00014-11-1-719.

1. Donoho DL (2006) Compressed sensing. *IEEE Transactions on Information Theory* 52(4):1289–1306.
2. Candès EJ, Romberg J, Tao T (2006) Robust uncertainty principles: Exact signal reconstruction from highly incomplete frequency information. *IEEE Transactions on Information Theory* 52(2):489–509.
3. Recht B, Fazel M, Parrilo P (2010) Guaranteed minimum-rank solutions of linear matrix equations via nuclear norm minimization. *SIAM Rev* 52(3):471–501.
4. Candès EJ, Eldar YC, Strohmer T, Voroninski V (2013) Phase retrieval via matrix completion. *SIAM Journal on Imaging Sciences* 6(1):199–225.
5. Candès EJ, Li X, Ma Y, Wright J (2011) Robust principal component analysis? *J ACM* 58(3):1–37. arXiv:0912.3599v1.
6. Schaeffer H, Caffisch R, Hauck CD, Osher S (2013) Sparse dynamics for partial differential equations. *Proc Natl Acad Sci USA* 110(17):6634–6639.
7. Nelson LJ, Hart G, Zhou F, Ozoliņš V (2013) Compressive sensing as a paradigm for building physics models. *Phys Rev B* 87(3):035125.
8. Prodan E, Kohn W (2005) Nearsightedness of electronic matter. *Proc Natl Acad Sci USA* 102(33):11635–11638.
9. Wannier GH (1937) The structure of electronic excitation levels in insulating crystals. *Phys Rev* 52(3):191–197.
10. Marzari N, Vanderbilt D (1997) Maximally localized generalized Wannier functions for composite energy bands. *Phys Rev B* 56(20):12847–12865.
11. Weinan E, Li T, Lu J (2010) Localized bases of eigensubspaces and operator compression. *Proc Natl Acad Sci USA* 107(4):1273–1278.
12. Donoho DL, Elad M (2003) Optimally sparse representation in general (non-orthogonal) dictionaries via  $l_1$  minimization. *Proc Natl Acad Sci USA* 100(5):2197–2202.
13. Lai R, Osher S (2013) A splitting method for orthogonality constrained problems. *J Sci Comput*, in press.
14. Osher S, Burger M, Goldfarb D, Xu J, Yin W (2005) An iterative regularization method for total variation-based image restoration. *Multiscale Model Simul* 4(2):460–489.
15. Yin W, Osher S, Goldfarb D, Darbon J (2008) Bregman iterative algorithms for  $l_1$ -minimization with applications to compressed sensing. *SIAM Journal on Imaging Sciences* 1(1):143–168.
16. Goldstein T, Osher S (2009) The split bregman method for  $l_1$ -regularized problems. *SIAM Journal on Imaging Sciences* 2(2):323–343.
17. Kronig RdeL, Penney WG (1931) Quantum mechanics of electrons in crystal lattices. *Proc R Soc Lond, A Contain Pap Math Phys Character* 130(814):499–513.
18. d'Aspremont A, El Ghaoui L, Jordan MI, Lanckriet G (2007) A direct formulation for sparse PCA using semidefinite programming. *SIAM Rev* 49(3):434–448.
19. Qi X, Luo R, Zhao H (2013) Sparse principal component analysis by choice of norm. *J Multivariate Anal* 114:127–160.
20. Ozoliņš V, Lai R, Caffisch R, Osher S (2013) *Compressed Plane Waves—Compactly Supported Multiresolution Basis for the Laplace Operator*, preprint.